Galactic cosmic ray and El Niño–Southern Oscillation trends in International Satellite Cloud Climatology Project D2 low-cloud properties

Nigel Marsh and Henrik Svensmark
Danish Space Research Institute, Copenhagen, Denmark

Received 30 August 2001; revised 5 September 2002; accepted 5 September 2002; published 29 March 2003.

[1] The recently reported correlation between clouds and galactic cosmic rays (GCR) implies the existence of a previously unknown process linking solar variability and climate. An analysis of the interannual variability of International Satellite Cloud Climatology Project D2 (ISCCP-D2) low-cloud properties over the period July 1983 to August 1994 suggests that low clouds are statistically related to two processes, (1) GCR and (2) El Niño–Southern Oscillation (ENSO), with GCR explaining a greater percentage of the total variance. Areas where satellites have an unobstructed view of low cloud possess a strong correlation with GCR, which suggests that low-cloud properties observed in these regions are less likely to be contaminated from overlying cloud. The GCR-low cloud correlation cannot easily be explained by internal climate processes, changes in direct solar forcing, or UV-ozone interactions. Instead, it is argued that a mechanism involving solar variability via GCR ionization of the atmosphere is consistent with these results. However, the results are marginal when including the recently extended ISCCP-D2 data covering the period until September 2001. This, we believe, is related to problems experienced with the ISCCP intercalibration between September 1994 and January 1995. *INDEX TERMS:* 0320 Atmospheric Composition and Structure: Cloud physics and chemistry; 1650 Global Change: Solar variability; 1620 Global Change: Climate dynamics (3309); 2104 Interplanetary Physics: Cosmic rays; *KEYWORDS:* low clouds, solar variability, cosmic rays, cosmic rays and clouds, ENSO and clouds, solar influence on climate

Citation: Marsh, N., and H. Svensmark, Galactic cosmic ray and El Niño–Southern Oscillation trends in International Satellite Cloud Climatology Project D2 low-cloud properties, *J. Geophys. Res.*, *108*(D6), 4195, doi:10.1029/2001JD001264, 2003.

1. Introduction

[2] Based on satellite observations, a link has been proposed between total cloud amount and the number of Galactic Cosmic Rays (GCR) received at Earth [*Svensmark and Friis-Christensen*, 1997; *Svensmark*, 1998]. Since clouds play an important role in the radiation budget of the atmosphere, by both reflecting solar radiation and trapping outgoing longwave radiation, the existence of a GCR-cloud link would introduce a previously unknown external forcing mechanism to the climate system. *Svensmark* [1998] speculated that a physical mechanism could involve the effects of GCR ionization on aerosol chemistry or the phase transitions of water vapor, which in turn would influence the activation of cloud droplets, and hence cloud radiative properties.

[3] However, beyond the GCR-total cloud correlation there is currently no experimental confirmation to suggest that such processes have had a discernible effect on cloud properties. This has lead to suggestions that the correlation is fortuitous and might better be explained by internal climate processes, e.g., El Niño–Southern Oscillation (ENSO), such that any agreement with cosmic rays is purely coincidental. As a result a number of questions have been raised as to the validity of the GCR-cloud link.

[4] *Kernthaler et al.* [1999] found no clear relationship between individual cloud types and GCR, which became further degraded with the inclusion of polar regions. However, their analysis relied on the individual cloud type derivations from the International Satellite Cloud Climatology Project monthly C2 data (ISCCP-C2) [*Rossow and Schiffer*, 1991] using an algorithm which was abandoned by ISCCP in 1990 due to its poor performance [*Klein and Hartmann*, 1993]. The reanalyzed D2 data (ISCCP-D2) using an improved algorithm [*Rossow et al.*, 1996], differs considerably from the ISCCP-C2 derivation of individual cloud types. The results of *Kernthaler et al.* [1999] cannot be reproduced using the ISCCP-D2 data, and it has been shown that there indeed exists a correlation between GCR and globally averaged ISCCP-D2 low cloud amount [*Marsh and Svensmark*, 2000a, 2000b]. *Kuang et al.* [1998] confirmed the GCR - total cloud correlation using the ISCCP-C2 data, but were unable to distinguish between the effects of GCR and ENSO on the mean cloud optical thickness. *Jorgensen and Hansen* [2000] raised a number of criticisms

0148-0227/03/2001JD001264

but of a more general nature which have been addressed in a comment by *Svensmark and Friis-Christensen* [2000]. Recently, *Kniveton and Todd* [2001] found a strong relationship between GCR and precipitation over southern oceans at mid to high latitudes. They suggest this is more consistent with changes in the global atmospheric electric circuit according to *Tinsley* [1996] rather than with tropospheric aerosols or ENSO. *Farrar* [2000] argues that trends in the globally averaged total cloud amount are the result of a composite of expected regional cloud responses to ENSO, and found little evidence to suggest a role for GCR. However, *Marsh and Svensmark* [2000b] have shown that the GCR-cloud correlation is limited to low cloud when using the ISCCP-D2 IR derivation of cloud properties, and that regions of the globe with a strong and significant correlation cannot easily be explained by internal climate processes. But the question remains, is the GCR - low cloud correlation an artifact which can be adequately explained by internal climate processes such as ENSO, or is it a signature of solar variability?

[5] Previously, discussions of a cosmic ray - low cloud link were based on ISCCP data available over the period July 1983–September 1994 [*Marsh and Svensmark*, 2000b]. An extension of ISCCP cloud data has recently been made available for the period January 1994 to September 2001 (January 1994–September 1994 were re-analyzed). However, between September 1994 and January 1995 there was a gap in available ISCCP calibration satellites. In section 3 it will be shown that following this gap, the ISCCP low-cloud data is found to deviate from an independent cloud data set obtained from the SSMI (Special Sensor Microwave Imager) instrument. The remainder of the paper will present a detailed analysis of the ISCCP-D2 low-cloud properties using point correlation and Empirical Orthogonal Function (EOF) analysis. The analysis is performed on two periods of the available cloud data; (1) July 1983–August 1994, and (2) July 1983–September 2001. In section 4 it will be shown that GCR and ENSO are the statistically dominant time series covarying with low clouds for period 1.

[6] Care must be taken in the interpretation of any low-cloud result when multi layer cloud is present as only the overlap portion of low cloud is viewed by satellite. Accounting for this effect by defining a "satellite view" of low clouds, it is possible to determine which regions of the globe reflect properties of low cloud with confidence. It is shown in section 5 that the GCR-cloud correlation is a robust feature of low-cloud properties for the period July 1983–August 1994.

[7] However, when the EOF analysis is repeated for period 2 these results are found to be marginal (see Appendix A). It is argued that this is the result of non-stationarities introduced to the cloud data after August 1994.

2. Data: ISCCP-D2, SSMI, GCR, and ENSO

[8] ISCCP-D2 provides monthly averaged satellite observations of cloud properties on an equal area grid (280 × 280 km) with each grid box containing up to 120 pixels (pixel sampling size ~25–30 km). A pixel is defined as cloudy if the infrared (IR-10.5 μm observed both day and night) or visible (VIS-0.7 μm observed day only) radiance differs from its clear sky value by more than a pre-calculated threshold. Cloud amount (CA) is then determined by the number of pixels in a grid box defined as cloudy. Relative uncertainties in radiance calibrations are <5% for VIS and <2% for IR [*Brest et al.*, 1997].

[9] Estimates of cloud top temperature and pressure (altitude) from the observed IR radiance for each cloudy pixel are made using an IR radiative transfer model, with an atmospheric temperature profile given by TOVS (TIROS Operational Vertical Sounder). When no cloud is detected, the radiative transfer model reports a surface temperature. Cloud top temperature (CT) and surface temperature (ST) are the monthly averaged temperatures for all cloudy and non-cloudy pixels respectively over each grid box. The estimate of cloud top pressure (altitude) for each IR detected cloudy pixel is used to define a cloud as low >680 hPa (<3.2 km), middle 680 – 440 hPa (3.2–6.5 km), or high <440 hPa (>~6.5 km). Thus, the monthly quantities of CA and CT for each grid box can additionally be obtained for low (CA_L, CT_L), mid (CA_M, CT_M) and high (CA_H, CT_H) cloud.

[10] The following analysis is restricted to clouds detected by IR radiance with its superior accuracy and coverage both spatially and temporally. However, the IR radiative transfer model assumes that all clouds are opaque, and thus does not allow for any transmitted radiance from below the cloud. While this is often true for low cloud, which tend to be optically thick, it is not generally the case for high optically thin cloud. This can lead to an over estimation of cloud top temperature and a biasing of high optically thin clouds to lower altitudes. Such problems can be solved if a clouds optical depth is known. ISCCP estimates cloud optical depth by modelling the effects of cloud scattering on VIS radiance and comparing the output with the satellite observations of VIS radiance. This leads to a visible adjustment to the IR cloud properties, but, a number of assumptions regarding the cloud droplet distribution must be made, which will additionally affect the accuracy at interannual time scales.

[11] There are three disadvantages with using the VIS radiance; (1) daylight observations only, (2) larger observational uncertainties and, (3) unrealistic assumptions regarding the cloud droplet distribution. Here it is arguably assumed that these disadvantages outweigh the benefits at interannual time scales, and the analysis is restricted to IR observations only.

[12] Independent observations of cloud amount can be obtained from the SSMI (Special Sensor Microwave Imager) instrument onboard the DMSP (Defence Meteorological Satellite Program) satellites. The SSMI instrument passively observes at 4 microwave wavelengths (19, 22, 37, and 85 GHz), which are able to penetrate cirrus and dust clouds, and thus have a less obscured view of liquid water clouds than ISCCP [*Ferraro et al.*, 1996]. The vertically integrated Liquid Water Path (LWP) is derived from an algorithm involving observations at all 4 wavelengths with a pixel resolution of 25km. SSMI cloud amount (SSMI-CA) is then defined as the number of pixels where LWP > 0.02mm within a 2.5° × 2.5° grid box. Monthly averages of SSMI-CA are available over the oceans from July 1987 - present (currently October 2001) with an 18 month gap between June 1990–December 1991 when the 85 GHz channel was shut down.

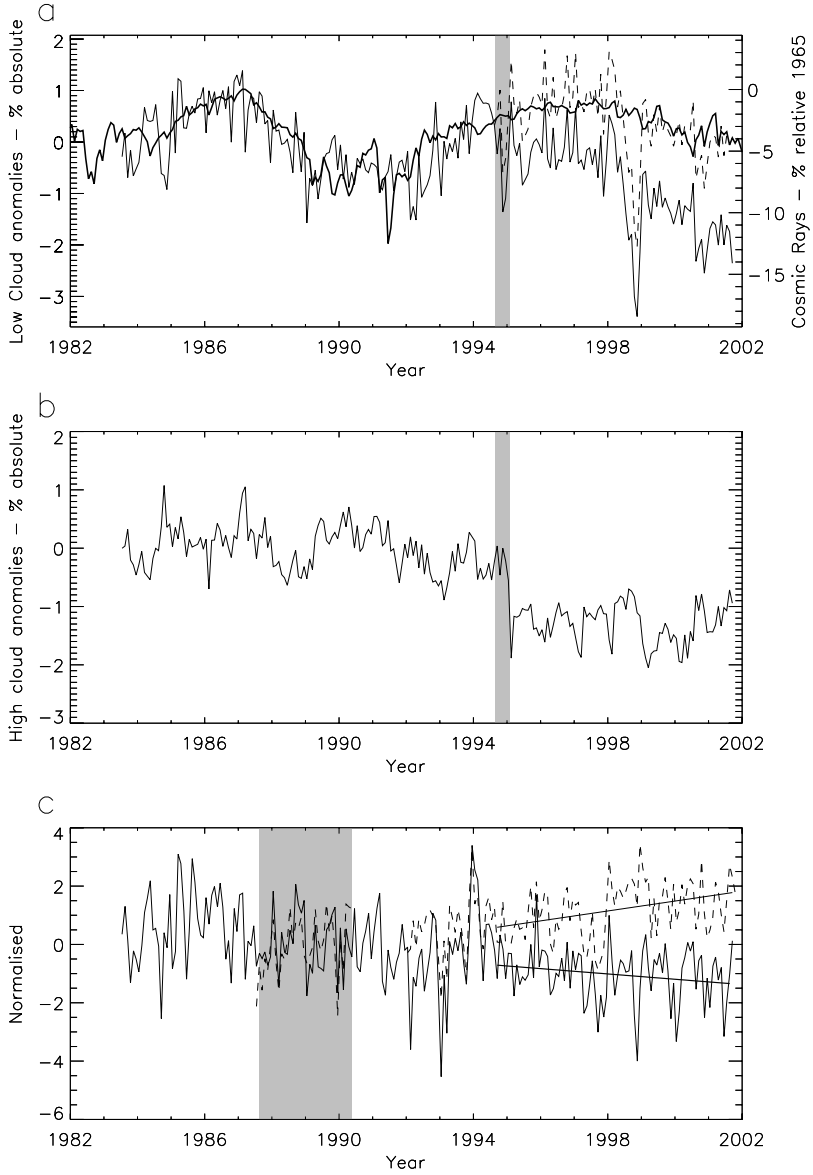

Figure 1. Monthly averages of cosmic rays (solid thick) and globally averaged anomalies (solid thin) of (a) ISCCP-CA_L, and (b) ISCCP-CA_H over the period of available ISCCP-D2 data. The dashed portion of the curve in (a) includes a drift term calculated by adding the difference between the linear trends seen in (c) to CA_L for each month. The anomalies are found by subtracting the climatic annual cycle for each month, averaged over the available period of ISCCP observations (July 1983–September 2001), before averaging over the globe. The shaded region in (a) and (b) denotes the gap in available ISCCP calibration satellites. (c) Spatial average of ISCCP-CA_L (solid) and SSMI-CA (dashed) over regions of significant correlation ($r > 0.5$, $p > 99\%$). Both ISCCP-CA_L and SSMI-CA have been normalized to their respective mean and variance over the highlighted period July 1987–June 1990. The solid straight lines represent the linear trends used in (a) for the respective curves starting July 1994.

[13] The benefit of SSMI over ISCCP is its ability to observe unobscured liquid water clouds. However, the SSMI instrument is onboard a single polar orbiting satellite which generates a global scene of Earth's cloud cover once a day. ISCCP uses radiances from a combination of geostationary and polar orbiting satellites that are intercalibrated using one of the polar orbiting satellites as a reference. A global cloud scene is produced every 3 hours, although monthly data is used in the following. Thus, where the intercalibration is stable, ISCCP has a better spatial and temporal resolution than SSMI. While SSMI data is useful to check for stability in long-term trends (performed over a limited area in the following), ISCCP data is more suitable for a detailed, global analysis.

[14] Cosmic Rays are represented by the number of neutron counts made at Huancayo (3km asl, 13GV cut-off rigidity). This signal contains both Galactic Cosmic Rays (GCR) and Solar Cosmic Rays (SCR), however at interannual timescales it is the GCR which are dominant. It is assumed here that GCR observed at Huancayo is represen-

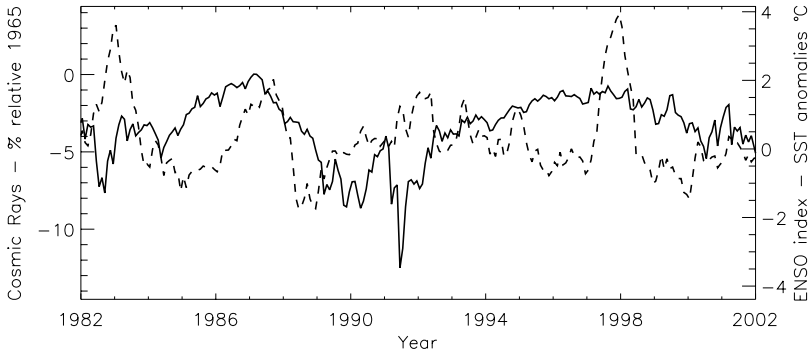

Figure 2. Monthly averages of cosmic rays (solid) and ENSO index (dashed). Cosmic Rays represent neutron counts observed at Huancayo (cut-off rigidity 12.91 GeV) and normalized to 1965. The ENSO index is given by NINO3 which is the average SST over the area 5°N–5°S, 150°–90°W.

tative of interannual trends globally [*Svensmark and Friis-Christensen*, 1997, Figure 1].

[15] The ENSO index is given by the average Sea Surface Temperatures (SSTs) anomalies over the region 5°N–5°S, 150°–90°W, known as NINO3 [*Wallace et al.*, 1998]. Situated in the eastern Pacific off the coast of Peru, the regions SSTs are governed by surface wind stress influencing the inclination of the thermocline in combination with other meteorological forcing and the impact of ocean dynamics. As surface easterlies weaken (strengthen) with the evolution of ENSO, so the inclination of the thermocline falls (rises) and the SSTs in the region defined NINO3 become warmer (cooler) [*Peixoto and Oort*, 1992]. Note NINO3 is anticorrelated with SST anomalies in the western Pacific over Indonesia.

3. GCR-Cloud Correlation

[16] Monthly averages of GCR (solid thick line) and the global average CA_L anomalies (solid thin line) are plotted together in Figure 1a over the period of available ISCCP-D2 observations (July 1983–September 2001). The correlation between CA_L and GCR for July 1983–Sept 1994 has previously been reported by *Marsh and Svensmark* [2000b] as r = 0.63 with significance p > 98% (r = 0.92, p > 99% for 12 month running means). (Note when calculating the significance, auto-correlations are taken into account by finding the effective number of degrees of freedom using the method of *Angell and Korshover* [1981]. Unless stated otherwise, further estimates of significance given below have been found in this way.) However, for the recently extended data the correlation and significance between CA_L and cosmic rays weakens, r = 0.26, p > 80% (r = 0.36, p > 80% for 12 month running means). The large decrease in CA_L in 1998 seen in Figure 1a, coincides with a sudden rise in middle cloud, partially obscuring the satellite view of low cloud below, which is probably related to the strong El Niño of 1998 (see Figure 2). Excluding the years after 1998 improves the correlation, r = 0.46, p > 96% (r = 0.72, p > 96% for 12 month running means). However, this does not account for the poor correlation over the remaining months between 1994–2001, which raises three possibilities; (1) there is no cosmic ray - low cloud link and the correlation between 1983–1994 is an artifact, (2) that the relationship exists only under certain climatic conditions which change in time and space, and (3) that there is a problem with the ISCCP detection of low cloud.

[17] During the period September 1994–January 1995 no polar orbiting satellite was available to ISCCP for maintaining a continuous intercalibration and it was necessary to perform an interpolation instead (see ISCCP homepage, ISCCP calibration coefficients, available at http://isccp.giss.nasa.gov/docs/calib.html). This may be responsible for introducing an artifical component into a number of ISCCP-D2 parameters, including CA_L and CA_T, after September 1994. In Figure 1b an offset is seen in high cloud amount, CA_H, towards the end of the calibration gap. A less dramatic offset is also present at around the same time in CA_L (Figure 1a). The sign of this offset rules out the possibility of CA_L merely responding to a change in the overlapping portion of CA_H. Whether a systematic change in the ISCCP cloud cover at all altitudes did occur or is due to some calibration artifact is a feature which will be discussed in detail in a future publication (N. D. Marsh and H. Svensmark, Possible artifacts in the ISCCP-D2 cloud data between 1994 and 1995, manuscript in preparation, 2003) (available at http://www.dsri.dk/~hsv). However, in the following a comparison between the long-term trends in CA_L and SSMI-CA are made to test for a possible systematic change in cloud cover.

[18] Liquid water clouds detected by SSMI will appear as either low or middle cloud types to ISCCP depending on their cloud top pressures. Since it is not possible for SSMI to distinguish between low and middle clouds, it is important to determine regions where ISCCP-CA_L and SSMI-CA are observing similar low cloud properties before investigating any possible deviations in long-term trends. These low-cloud-dominant regions are selected where a significant positive correlation (r > 0.5, p > 99%) is found between CA_L and SSMI-CA on a 2.5° × 2.5° degree grid. Limiting the period over which the correlation is found to July 1987–June 1990 (36 months) provides a unique opportunity to independently test for any disagreements in the long term trends after January 1992. Figure 1c shows the temporal evolution for the normalized average of CA_L and SSMI-CA over these low-cloud-dominant regions. Both of these regionally averaged quantities have been normalized to their respective mean and variance found over the highlighted period, July 1987–June 1990. Per definition there is a good agreement over the period used to select these

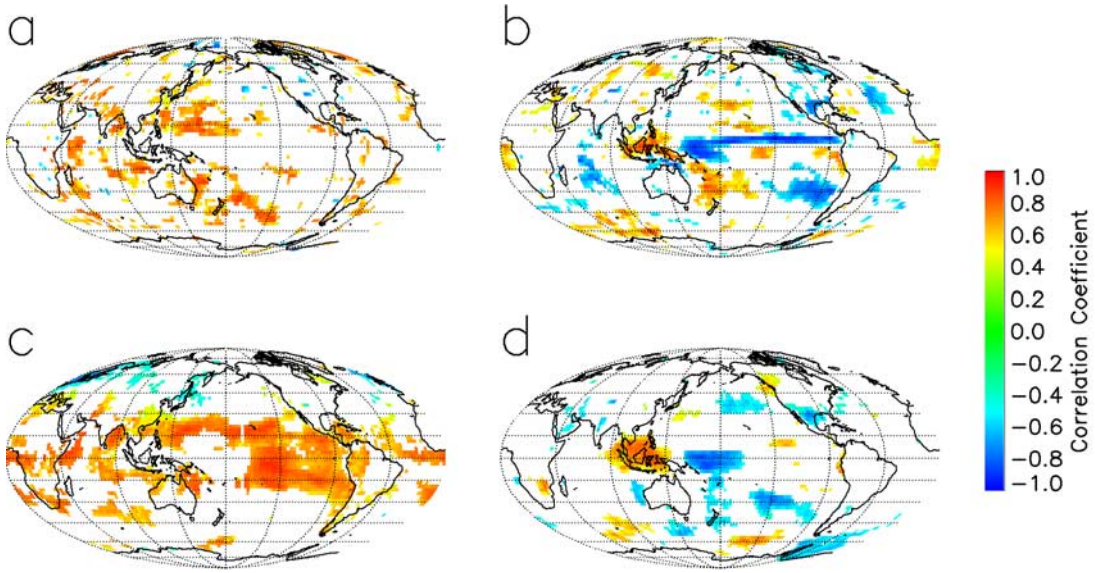

Figure 3. Point correlation maps for the period July 1983–August 1994 between; (a) GCR and CA_L, (b) ENSO and CA_L, (c) GCR and CT_L, and (d) ENSO and CT_L. The correlation coefficient, r, is calculated from the 12 month running means at each grid box. Only pixels possessing a significant correlation, p > 95% are colored.

regions. However, the period starting January 1992 is independent of this pre-selection, and the good agreement until the middle of 1994 confirms that ISCCP and SSMI are detecting the same relative low-cloud properties over these regions. After 1994, the two curves diverge displaying differing trends in their respective long-term means, while still maintaining a good correlation at shorter time scales (<∼1 year). This divergence occurs at roughly the same time that ISCCP experiences problems with the satellite intercalibation.

[19] Figure 1c suggests that there are long-term drifts in at least one of the satellite data sets. Although it is not possible to resolve these discrepancies at present, uncertainties in the drift can be evaluated from the difference between ISCCP and SSMI after June 1994. One limit of uncertainty can be seen in Figure 1a where such a correction is included after August 1994 (dashed curve), and the agreement with cosmic rays is somewhat improved, r = 0.60, p > 99% (r = 0.89, p > 99% for 12 month running means). While not a proof that the correlation still holds, the disagreement between ISCCP-CA_L and SSMI-CA and ISCCP's intercalibration problem does indicate that the uncertainties in the long-term trends of cloud properties for the period after August 1994 are large.

4. Analysis of Period July 1983 to August 1994

[20] From Figure 2 it can be shown that GCR and the ENSO index are orthogonal, which is reflected in their correlation coefficient, r = 0.01. This suggests that it is unlikely ENSO could explain the globally averaged CA_L, however, it does not rule out any regional influences.

[21] Point correlation maps of CA_L with GCR and ENSO for each grid box can be seen in Figures 3a and 3b respectively. Only grid points possessing a significant correlation, P > 95%, are colored. Regions of strong GCR correlation are generally positive, while regions of strong ENSO correlation are both positive and negative with roughly equal area weight. Thus when taking a global average of CA_L the ENSO signal will be averaged out, while the GCR signal survives, as can be seen in Figure 1a. Also shown in Figures 3c and 3d, are the point correlation maps of CT_L with GCR and ENSO. Again, only grid points possessing a significant correlation, p > 95 are colored. Note that in Figures 3a and 3c, the probability of obtaining the observed fractions of the globe with r > 0.6 by chance has previously been shown to be $<10^{-3}$ from an ensemble of Monte Carlo simulations [*Marsh and Svensmark*, 2000b]. For both CA_L and CT_L regions correlated with GCR are complimentary to regions correlated with ENSO such that the correlation maps are almost orthogonal (where the dot product gives 89° for CA_L and 97° for CT_L). These orthogonality properties suggest that an Empirical Orthogonal Function (EOF) analysis would be appropriate.

[22] If GCR and ENSO influences are dominant processes related to low-cloud properties at interannual time scales they should be captured by the leading components of an EOF analysis. Here the data set is decomposed into a linear set of independent correlation patterns (spatial components) by rotating the correlation matrix to maximize the fraction of total variance captured by each pattern under the condition of orthogonality. It is assumed that those patterns capturing the largest significant variance are the result of some physical process [*Preisendorfer*, 1988]. In the current analysis, this is beneficial for two reasons: (1) The EOF decomposition does not involve the ENSO or GCR signals directly, thus if captured by the leading EOF components it would provide independent evidence that these processes play a significant role in low-cloud variability, and (2) if this is the case then it would give an estimate of the relative contribution from GCR and/or ENSO to the total variance in the observed low-cloud properties.

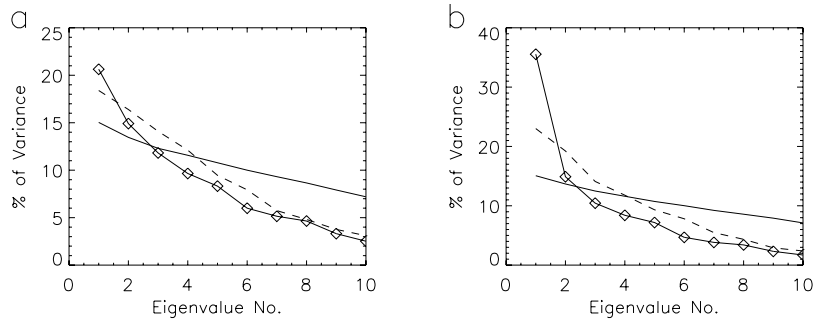

Figure 4. The percentage of total variance captured by each of the first 10 Eigenvalues (black diamonds) for (a) CA_L, and (b) CT_L. In both plots the 95% significance levels obtained from a Monte Carlo (Rule N) simulation [*Preisendorfer*, 1988] are given, where the thin line assumes a gaussian distribution with 11 dof, and the dashed line is generated by randomizing the Fourier phases of the cloud data (see text). Randomizing the Fourier phases is a stricter test which accounts for any autocorrelations that are present.

[23] The leading Eigenvalues, obtained from a correlation matrix calculated from 12 month running means (11 independent points) of CA_L and CA_T, are seen in Figure 4. To determine which Eigenvalues are significant at p > 95%, Monte Carlo simulations have been used to generate an ensemble of correlation matrices from which their respective Eigenvalues are found. The 100 members of each ensemble consisted of N independent artificial time series, where N ($\sim$160) is the spatial degree of freedom, as given by *Marsh and Svensmark* [2000b]. Two distinct assumptions are used to generate the artifical time series. In the first case, the artificial time series are drawn from a gaussian distribution with 11 temporal degrees of freedom (Figure 4, blue lines). In the second case, the artificial time series are generated by Fourier transforming the real cloud data, randomizing the phases, and then Fourier transforming back (Figure 4, green lines). Randomizing the Fourier phases is a stricter test which accounts for any autocorrelations that are present. Figures 4a and 4b reveals that under the first assumption the leading two Eigenvalues are significant at p > 95%, but under the stricter second assumption only the first Eigenvalue is significant at p > 95% while the second Eigenvalue is marginal.

[24] The spatial components of the first two leading EOFs, i.e., those capturing the greatest percentage of variance, for CA_L and CT_L are seen in Figure 5, clearly there are similarities with the correlation maps of Figure 3. Each spatial component has been renormalized so that its modulus is equal to that for the equivalent correlation map of Figure 3, allowing for the same color scale to be used for ease of comparison.

[25] The corresponding temporal components (normally referred to as principle components), T, are found by projecting the matrix of original low-cloud observations, D, onto each spatial component, A, in turn:

$$T = DA \tag{1}$$

[26] The temporal components for the first two leading EOFs of CA_L and CA_T are seen in Figure 6 together with the

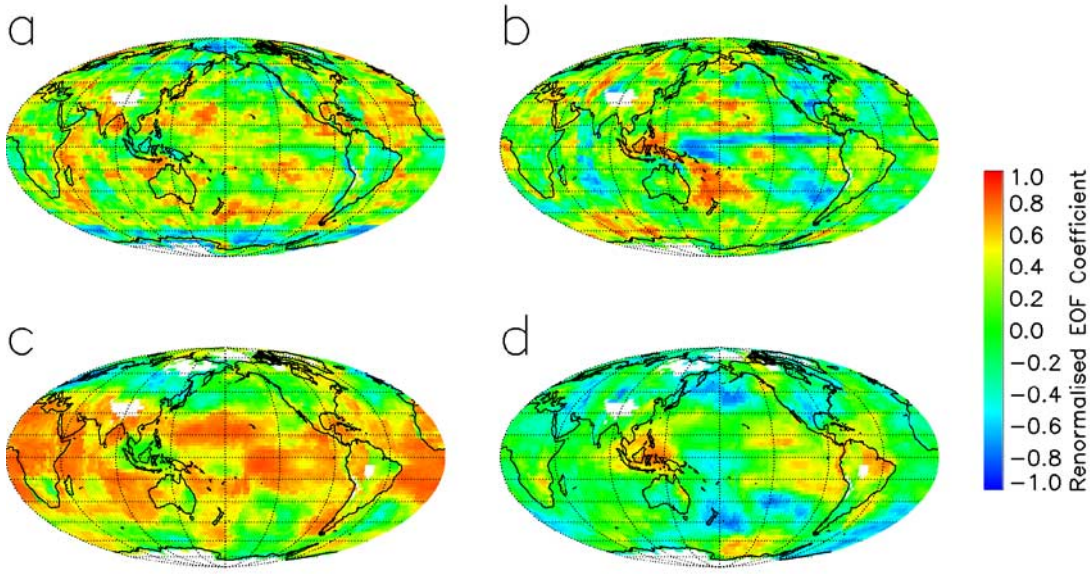

Figure 5. Spatial components of the leading 2 EOFs for CA_L (a) and (b), and CT_L (c) and (d). The color scale is the same as in Figure 3. The modulus length of each map has been renormalized to the equivalent correlation map in Figure 3 for ease of comparison. White pixels indicate regions with either no data or an incomplete monthly time series.

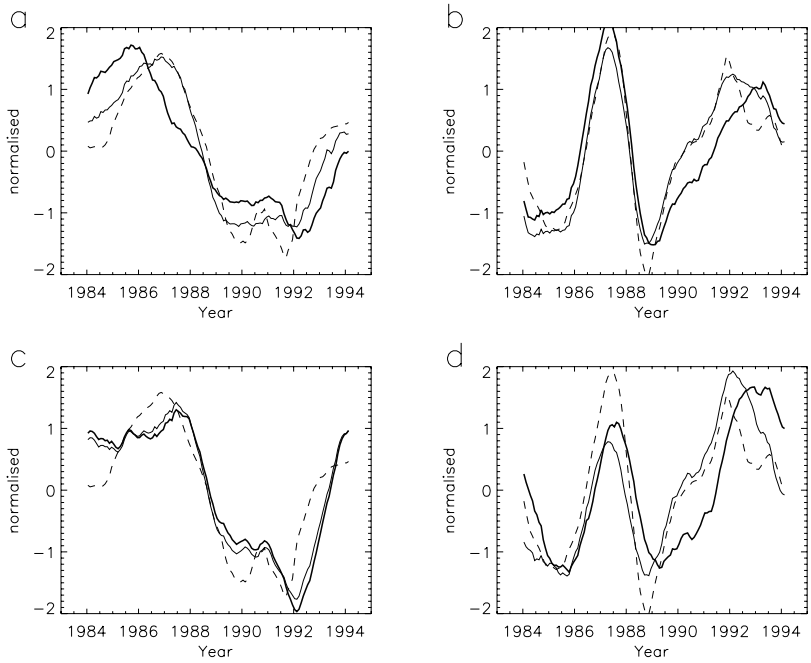

Figure 6. Temporal components (solid thick) of the first two EOFs obtained from CA_L and CT_L. Figures 6a–6d are respectively related to the spatial components in Figure 5, i.e., temporal components of the leading 2 EOFs for CA_L (a) and (b), and CT_L (c) and (d). The dashed curves represent GCR in (a) and (c), and ENSO in (b) and (d). Also plotted are the temporal components (solid thin) obtained when projecting the cloud properties onto the correlation maps of Figure 3 (see text).

GCR and ENSO signals. The agreement is reasonable although there are some differences, notably the timing of the maxima in 1987 for GCR and 1991/92 for ENSO. These differences are mainly the result of the strict orthogonality requirement which will tend to rotate the spatial components relative to the correlation maps of Figure 3, thus affecting the temporal components. To emphasize this point Figure 6 also includes the temporal components generated when projecting the low-cloud observations onto the correlation maps of Figure 3. As might be expected a much better agreement between these temporal components and the GCR and ENSO time series is seen. Despite these differences there is a remarkable similarity in regions displaying strong positive or negative correlation in Figures 3 and 5. This suggests that the first two leading EOFs of CA_L and CT_L could be attributed to GCR and ENSO. The estimated percentage of variance captured by these respective EOFs is found to be; 20.6% and 14.9% of CA_L variance, and, 35.5% and 14.9% of CT_L variance. This indicates that the GCR signal is more dominant in low-cloud interannual variability than ENSO. However, before there can be confidence that this is a real property of low cloud, effects influencing the satellite view of the lower atmosphere must be considered.

5. Satellite View of Low Clouds

[27] Since satellites observe the Earth's cloud cover from above their ability to observe variability in low clouds can be hindered by the presence of overlying cloud [*Weare*, 2000]. To test whether this effect will influence the interpretation of the above results a "satellite view" of the atmosphere not obscured by middle and high clouds in each grid box is defined as:

$$SAT_{lowview} = 1 - (CA_M + CA_H) = CLR + CA_L \quad (2)$$

where CLR represents the fraction of clear sky, i.e., $1 - (CA_L + CA_M + CA_H)$. Using this definition for $SAT_{lowview}$, the influence of middle and high cloud amount on satellite detection of low cloud can be investigated. A strong positive correlation coefficient, i.e. $r \sim 1$, between $SAT_{lowview}$ and CA_L, would indicate that the satellites view of low-cloud variability is hindered by overlying cloud, and that trends in low-cloud properties reflect the inverse trends from cloud above. A lack of correlation, $r \sim 0$ indicates that upper cloud variability is not limiting the ability of the satellites to capture properties of low cloud. By selecting a minimum level of significant correlation, r_{limit}, each grid box can be designated as contaminated where $r \geq r_{limit}$. Those grid boxes not contaminated are assumed to display the properties of real low cloud. The determination of r_{limit} is an important feature of this analysis and is defined here where the significance p > 99% and the fraction of variance, r^2, is $\geq$ 50%, i.e., $r_{limit} = 0.7$ for both annual and monthly averages.

[28] Figure 7 is a replica of Figures 3a and 3c but where regions colored white now indicate grid boxes ($r \geq 0.7$) contaminated with overlying cloud. Those regions remaining include the significant correlation with GCR for both CA_L and CT_L, while contaminated regions include areas where a strong correlation was previously found with ENSO (compare Figures 3b and 3d). This latter feature can be understood from the fact that ascending air motion, responsible for the creation of high cloud, is generally dependent

on surface temperature, in particular SSTs in tropical regions [*Kent et al.*, 1995]. Thus atmospheric convection, and hence high cloud, will evolve with ENSO as the SSTs of the Pacific wax and wane. The presence of a strong ENSO signal in regions of high cloud will affect the satellite view of any low cloud below, resulting in a high correlation coefficient between CA_L and $SAT_{lowview}$, and CA_L and ENSO. The fact that the GCR - low cloud correlation survives at p > 95% significance suggests it is a feature of real low cloud, and that cloud processes influenced by GCR are unlikely to be the result of large-scale dynamical changes in the atmosphere as with ENSO.

6. Discussion and Conclusions

[29] The interannual variability of ISCCP-D2 low-cloud properties between July 1983–August 1994 has been shown to be statistically related to two processes, GCR and ENSO. ENSO is known to have a strong effect on high cloud properties over time scales up to decades. The ENSO signal captured by ISCCP satellite observations of low cloud appears to be the result of overlapping from clouds above. The GCR-low cloud link, on the other hand, is complimentary to the ENSO signal, and is strongest in regions where satellites have an un-obstructed view of low cloud. This finding suggests that the GCR - low cloud correlation over the period July 1983–August 1994 is based on real cloud properties.

[30] However, this result is considerably weakened when analyzing the full period (July 1983–Sept. 2001) of available data (see Appendix A). This is due to non-stationarities in the cloud data resulting from either changes in the underlying physical processes, such as ENSO, or the introduction of artifacts due to calibration problems. The nature of the offset in CA_L (Figure 1a) around 1994/1995 and it's presence in a number of other cloud parameters, e.g. CA_H Figure 1b, suggests to us that this may be related to the calibration gap experienced by ISCCP. This does not mean that the ISCCP data either side of this offset is of poor quality, but that the inclusion of the offset will render artificial any time series analysis. As a result we have focused on the period July 1983–August 1994.

[31] Although a correlation exists between GCR and low-cloud properties, a physical mechanism explaining the role of GCRs in cloud formation is still speculative. GCRs are negatively correlated with solar irradiance, which has led to suggestions that changes in irradiance may explain the GCR-cloud correlation [*Udelhofen and Cess*, 2001]. The correlation coefficient obtained between CA_L and solar irradiance for 12 month running means prior to the El Niño in 1998 is, r = −0.73, p > 96%, which is not significantly different from that obtained over the same period when correlating with GCR, r = 0.72, p > 96%. Changes in solar irradiance could modulate cloud properties through changes in atmospheric circulation either directly or indirectly via UV effects in the stratosphere. Direct changes are probably too small to influence atmospheric circulation significantly, however, model studies have shown that solar variability of UV radiation can affect temperatures in the stratosphere through absorption by ozone, and has the potential to influence the large-scale dynamics of the troposphere [*Haigh*, 1996; *Shindell et al.*, 1999]. Such a mechanism would be expected to have its strongest impact on convective high cloud, similar to the effect of ENSO, but forced from above. *Udelhofen and Cess* [2001] have shown that ground based observations of total cloud cover over the US possess a solar signal, which they suggest could be due to the role of UV induced circulation changes influencing mainly high cloud with a weaker effect lower down in the troposphere. However, no solar signal was found in an analysis of ISCCP-D2 high or middle cloud [*Marsh and Svensmark*, 2000b] suggesting that for ISCCP clouds at least the GCR - low cloud link cannot easily be explained by circulation changes, and a mechanism restricted to the lower troposphere is required. As discussed by *Marsh and Svensmark* [2000b] recent theoretical studies indicate that ionization could be a limiting process for aerosol production in the lower maritime atmosphere [*Yu and Turco*, 2000a, 2000b], and that systematic variations in GCR ionization could affect atmospheric aerosols acting as cloud condensation nuclei (CCN) for cloud droplets, and hence low-cloud properties [*Yu and Turco*, 2001]. Under these conditions, an increase in GCR would lead to an increase in aerosol and hence a decrease in cloud droplet sizes. *Ferek et al.* [2000] have shown that an increase in aerosol due to ship exhaust can lead to drizzle suppression which has implications for cloud lifetimes. If ionization from GCR can be shown to have a similar affect on aerosol sizes, and subsequently prolong a clouds lifetime, it would be consistent with the GCR - CA_L correlation reported here. However, it should be noted that ship tracks are a large perturbation locally, whereas a possible GCR/CCN mechanism will be a small perturbation globally.

[32] The connection between GCR-CCN-CT_L is not so clear. Changes in ISCCP's CT_L can be the result of variability in cloud top height, cloud optical depth, or some undetected

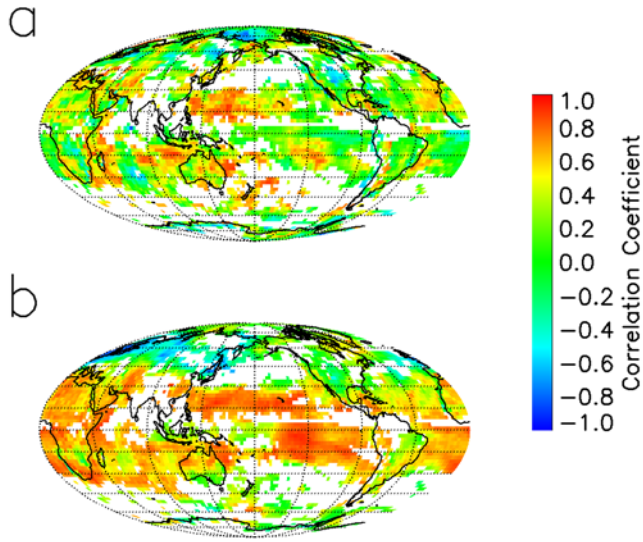

Figure 7. Point correlation maps where the correlation coefficient at each grid box is found between; (a) GCR and CA_L, (b) GCR and CT_L, as in Figures 3a and 3c, but where regions colored white now indicate grid boxes contaminated with overlying cloud (see text).

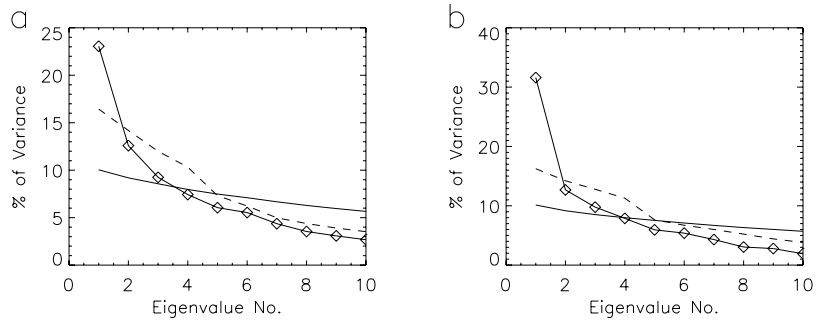

Figure A1. The percentage of total variance captured by each of the first 10 Eigenvalues (black diamonds) found for (a) CA_L, and (b) CT_L over the period July 1983–September 2001. In both plots the 95% significance levels obtained from a Monte Carlo (Rule N) simulation [*Preisendorfer*, 1988] are given, where the thin line assumes a gaussian distribution with 18 dof, and the dashed line is generated by randomizing the Fourier phases of the cloud data (see section 3). Randomizing the Fourier phases is a stricter test which accounts for any autocorrelations that are present.

changes in the atmospheric profile as measured by TOVS. The direct response in cloud optical depth to an increase (decrease) in GCR/CCN will be an increase (decrease) in cloud albedo affecting the reflected VIS radiation, and a decrease (increase) in cloud transmissivity affecting the IR radiation leaving cloud tops. Under ISCCP's assumption of opaque clouds (i.e., no transmission), an increase (decrease) in GCR/CCN will lead to an apparent decrease (increase) in CT_L, which is inconsistent with the positive correlation found between GCR-CT_L. However, this does not account for changes in CCN affecting indirect processes or feedbacks involving internal cloud dynamics. A further possibility is that an artificial signal enters CT_L that is the result of undetected changes in the atmospheric profile measured by TOVS [*Wang et al.*, 1999]. Currently, it is an open question whether the GCR-CT_L correlation is the result of a realistic process or is an artifact. Despite this lack of uncertainty the GCR-CCN-cloud link is an appealing mechanism, which requires confirmation by experiment to determine it's potential implications for climate.

[33] There is a need to understand the implications of solar variability on climate, whether it be through direct solar irradiance, UV-ozone interactions, or cosmic ray ionization. The results presented here lend further support to the idea that at interannual timescales, solar variability has influenced low cloud. The apparent lack of a solar signal in upper level clouds points towards a mechanism restricted to the lower troposphere. Such a feature is more consistent with an effect from cosmic ray ionization-aerosol interactions rather than UV-ozone influences on atmospheric circulation.

Appendix A: Analysis of Period July 1983 to September 2001

[34] In this appendix the EOF analysis in section 3 is repeated for all available ISCCP-D2 data covering the

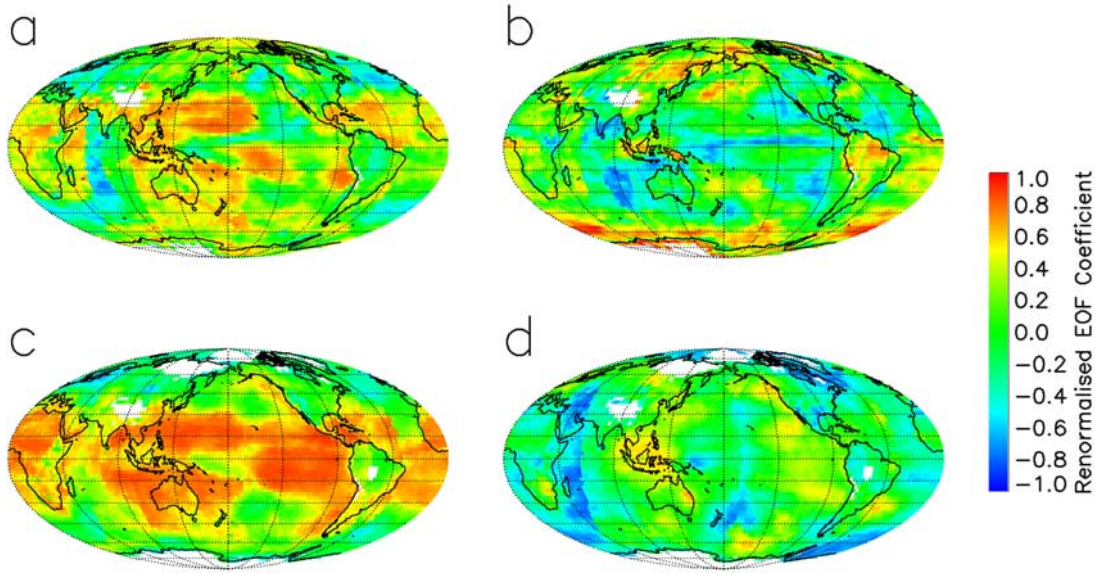

Figure A2. Spatial components of the leading 2 EOFs for CA_L (a) and (b), and CT_L (c) and (d) for the period July 1983 to Sept. 2001. The color scale is the same as in Figure 5. The modulus length of each map has been renormalized to the equivalent spatial components in Figure 5 so that the same color scale can be used for ease of comparison. White pixels indicate regions with either no data or an incomplete monthly time series.

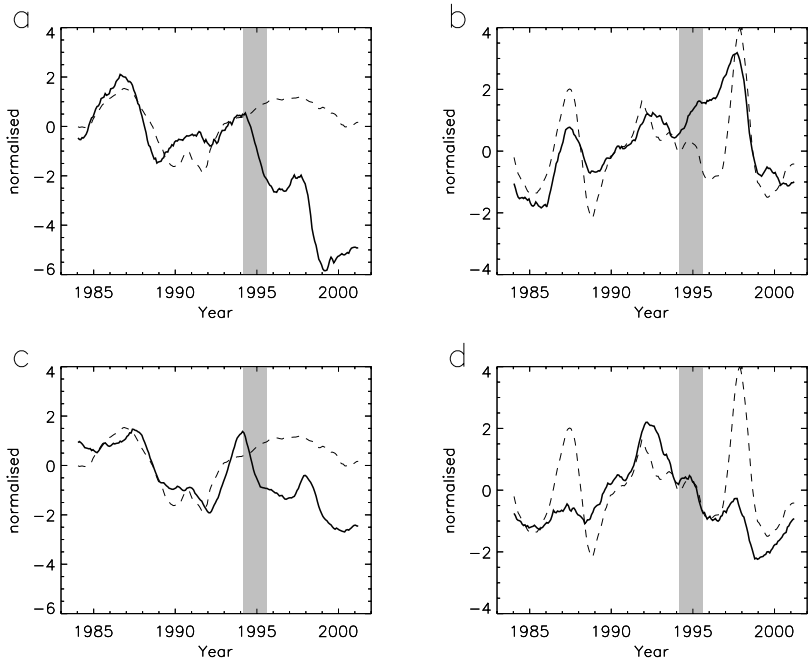

Figure A3. Temporal components (solid thick) of the first two EOFs obtained from CA_L and CT_L for the period July 1983 to Sept. 2001. Figures A3a–A3d are respectively related to the spatial components in Figure A2, i.e., temporal components of the leading 2 EOFs for CA_L (a) and (b), and CT_L (c) and (d). The dashed curves represent GCR in (a) and (c), and ENSO in (b) and (d). The shaded region highlights the period potentially influenced by the calibration gap; note since 12 month running means are being used this region is increased by ±6 months.

period July 1983–September 2001. This period includes the calibration gap experienced by ISCCP between September 1994–January 1995. It was noted in section 3 and Figures 1a and 1b that various IR cloud parameters display an offset around or after this period. This is either the result of a real systematic change in global cloud properties, or a calibration artifact. Such an offset will introduce a non-stationary component into the time series which can be detrimental for an EOF analysis. However, for completeness sake we have chosen to include here the EOF analysis performed on the full data and highlight the differences with the results of section 3. In the following, Figures A1–A3 are equivalent to Figures 4–6 in section 3.

[35] The leading Eigenvalues shown in Figure A1 and the significance at p > 95% are found in the same way as for Figure 4, section 3. Three eigenvalues are found to be significant assuming a gaussian distribution, but when accounting for autocorrelations only the first eigenvalue is significant at p > 95% while the second is marginal. The amount of variance captured by the first two EOFs is found to be; 23.1% and 12.6% of CA_L variance, and, 31.6% and 12.7% of CT_L variance.

[36] The spatial components of the first two leading EOFs for CA_L and CT_L are seen in Figure A2. The general features appear similar to the spatial components of Figure 5, although on closer inspection there is an element of "mixing" between the spatial components and a weakening of the dominant areas captured, particularly in the second EOF (compare (b) and (d) in Figures A2 and 5). These differences are due to a rotation of the EOF vectors derived from the extended time series. Such features are expected when the time series are non-stationary.

[37] The temporal components in Figure A3 of CA_L and CT_L indicate that the agreement with GCR for the first EOF is reasonable up to 1994, as in Figure 6, but thereafter breaks down. The temporal components for the second EOF show some resemblance to the ENSO index, but not to the same extent as seen in Figures 5b and 5d for the shorter period. Again this is expected when the time series are non-stationary. For ISCCP-D2 cloud properties this could be the result of either non-stationary physical processes or an artifact due to the calibration gap. The former is a likely explanation for the differences relating to the ENSO index since the atmospheric response to the strong El Niño of 1998 was observed to be considerably different to that of the El Niño in 1987 [*Cess et al.*, 2001]. It is quite remarkable that the leading EOF captures a sudden drop in both CA_L and CT_L at the time of the calibration gap. This of course may be a real feature and its timing just coincidence, but the fact that the drop is apparent in a number of other parameters, e.g., high cloud amount Figure 1b, suggests to us that this might be an artifact due to the calibration gap.

[38] **Acknowledgments.** The Huancayo neutron counts were supplied by University of Chicago, "National Science Foundation grant ATM-9912341."

References

Angell, J. K., and J. Korshover, Comparison between sea surface temperature in the equatorial eastern Pacific and United States surface temperatures, *J. Appl. Meteorol.*, *20*, 1105–1110, 1981.

Brest, C., W. B. Rossow, and M. D. Roiter, Update of radiance calibrations for ISCCP, *J. Atmos. Oceanic Technol.*, *14*, 1091–1109, 1997.

Cess, R. D., M. Zhang, B. A. Wielicki, D. F. Young, X.-L. Zhou, and Y. Nikitenko, Update of radiance calibrations for ISCCP, *J. Clim.*, *14*, 2129–2137, 2001.

Farrar, P., Are cosmic rays influencing oceanic cloud coverage-or is it only El Niño?, *Clim. Change*, *47*, 7–15, 2000.
Ferek, R. J., et al., Drizzle suppression in ship tracks, *J. Atmos. Sci.*, *57*(16), 2707–2728, 2000.
Ferraro, R., F. Weng, N. Grody, and A. Basist, An eight-year (1987–1994) time series of rainfall, snow cover, and sea ice derived from SSM/I measurements, *Bull. Am. Meteorol. Soc.*, *77*, 891–906, 1996.
Haigh, J. D., The impact of solar variability on climate, *Science*, *272*, 981–984, 1996.
Jorgensen, T., and A. Hansen, Comment on "Variation of cosmic ray flux and global cloud coverage: A missing link in solar-climate relationships" by Herik Svensmark and Eigil Friis-Christensen, *J. Atmos. Sol. Terr. Phys.*, *62*, 73–74, 2000.
Kent, G. S., E. R. Williams, P. H. Wang, M. P. McCormick, and K. M. Skeens, Surface temperature related variations in tropical cirrus cloud as measured by SAGE II, *J. Clim.*, *8*, 2577–2594, 1995.
Kernthaler, S., R. Toumi, and J. Haigh, Some doubts concerning a link between cosmic rays fluxes and global cloudiness, *Geophys. Res. Lett.*, *26*, 863–866, 1999.
Klein, S., and D. Hartmann, Spurious changes in the ISCCP data set, *Geophys. Res. Lett.*, *20*, 455–458, 1993.
Kniveton, D. R., and M. C. Todd, On the relationship of cosmic ray flux and precipitation, *Geophys. Res. Lett.*, *28*, 1527–1530, 2001.
Kuang, Z., Y. Jiang, and Y. Yung, Cloud optical thickness variations during 1983–1991: Solar cycle or ENSO?, *Geophys. Res. Lett.*, *25*, 1415–1418, 1998.
Marsh, N. D., and H. Svensmark, Cosmic rays, clouds and climate, *Space Sci. Rev.*, *94*, 215–230, 2000a.
Marsh, N. D., and H. Svensmark, Low cloud properties influenced by cosmic rays, *Phys. Rev. Lett.*, *85*, 5004–5007, 2000b.
Peixoto, J. P., and A. H. Oort, *Physics of Climate*, Am. Inst. of Phys., New York, 1992.
Preisendorfer, R. W., *Principle Component Analysis in Meteorology and Oceanography*, Elsevier Sci., New York, 1988.
Rossow, W. B., and R. A. Schiffer, ISCCP cloud data products, *Bull. Am. Meteorol. Soc.*, *72*, 2–20, 1991.
Rossow, W. B., A. W. Walker, D. E. Beuschel, and M. D. Roiter, International Satellite Cloud Climatology Project (ISCCP): Documentation of New Cloud Datasets, *WMO/TD-No. 737*, World Meteorol. Organ., Geneva, 1996.
Shindell, D., D. Rind, N. Balabhandran, J. Lean, and P. Lonergan, Solar cycle variability, ozone, and climate, *Science*, *284*, 305–308, 1999.
Svensmark, H., Influence of cosmic rays on climate, *Phys. Rev. Lett.*, *81*, 5027–5030, 1998.
Svensmark, H., and E. Friis-Christensen, Variation of cosmic ray flux and global cloud coverage: A missing link in solar-climate relationships, *J. Atmos. Sol. Terr. Phys.*, *59*, 1225–1232, 1997.
Svensmark, H., and E. Friis-Christensen, Reply to comments on "Variation of cosmic ray flux and global cloud coverage: A missing link in solar-climate relationships,"*, J. Atmos. Sol. Terr. Phys., 62*, 79–80, 2000.
Tinsley, B. A., Correlations of atmopsheric dynamics with solar wind-induced changes in air-earth current density into cloud tops, *J. Geophys. Res.*, *101*, 29,701–29,714, 1996.
Udelhofen, P., and R. Cess, Cloud cover variations over the United States: An influence of cosmic rays or solar variability?, *Geophys. Res. Lett.*, *28*, 2617–2620, 2001.
Wallace, J. M., E. M. Rasmusson, T. P. Mitchell, V. E. Kousky, E. S. Sarachik, and H. von Storch, On the structure and evolution of ENSO-related climate variability in the tropical Pacific: Lessons from TOGA, *J. Geophys. Res.*, *103*, 14,241–14,260, 1998.
Wang, J., W. B. Rossow, T. Uttal, and M. Rozendaal, Variability of cloud vertical structure during ASTEX observed from a combination of rawinsonde, radar, ceilometer, and satellite, *Mon. Weather Rev.*, *127*, 2484–2502, 1999.
Weare, B. C., Near global observations of low clouds, *J. Clim.*, *13*, 1255–1268, 2000.
Yu, F., and R. P. Turco, Ultrafine aerosol formation via ion-mediated nucleation, *Geophys. Res. Lett.*, *27*, 883–886, 2000a.
Yu, F., and R. P. Turco, Galactic cosmic ray ionization, aerosol formation, and CN/CCN abundance in the troposphere, *Eos Trans. AGU*, *81*(9), Spring Meet. Suppl., S158, 2000b.
Yu, F., and R. P. Turco, From molecular clusters to nanoparticles: Role of ambient ionization in tropospheric aerosol formation, *J. Geophys. Res.*, *106*, 4797–4814, 2001.

N. Marsh and H. Svensmark, Danish Space Research Institute, Juliane Maries Vej 30, DK-2100, Copenhagen Ø, Denmark. (ndm@dsri.dk; hsv@dsri.dk)